

Structure, Potentiometric and Thermodynamic Studies of N-Acryloyl-4-amino salicylic acid and Its Metal Complexes in Monomeric and Polymeric Forms

El-Binary AA¹, Ghoneim MM², Diab MA¹, El-Sonbati AZ¹ and Serag LS¹

¹Chemistry Department, Faculty of Science, Damietta University, Damietta 34517, Egypt

²Chemistry Department, Faculty of Science, Tanta University, Tanta, Egypt

Abstract

N-Acryloyl-4-aminosalicylic acid (AAS) was synthesized and characterized using different spectroscopic techniques. The geometrical structures of the ligand are carried out by HF method with 3-21G basis set. The proton-ligand dissociation constants of AAS and its metal stability constants with (Mn²⁺, Co²⁺, Ni²⁺ and Cu²⁺) have been determined potentiometrically in monomeric and polymeric forms using 2,2'-azobisisobutyronitrile as initiator. The potentiometric studies were carried out in 0.1 M (KCl) and 20% (by volume) ethanol-water mixture. The effect of temperature was studied at (298, 308 and 318 K) and the corresponding thermodynamic parameters (ΔG , ΔH and ΔS) were derived and discussed. The dissociation process is non-spontaneous, endothermic and entropically unfavorable. The formation of the metal complexes has been found to be spontaneous, endothermic and entropically favorable.

Keywords: N-Acryloyl-4-aminosalicylic acid; Molecular structure; Potentiometry; Thermodynamics

Introduction

Polymer complexes have been given a great deal of attention in recent years. The formation of chelates by polymers has widely been used for speciation [1], concentration, separation [2] and recovery [3] of metal ions. Stability constants are key parameters for the investigation of equilibria in solution and are very important in many fields such as industrial chemistry [4], environmental studies [5], as well as medicinal [6] and analytical chemistry. Potentiometric method is used to determine the average number of ligands coordinated with metal ion and, further, calculation the stability constants of polymer-metal complexes [7-10].

Salicylic acid and its derivatives are also biologically important ligands, a well known and widely used derivative, aspirin, reduces the risk of many diseases associated with ageing and is used in the treatment of rheumatic fever, pain, the prevention of thrombosis in vascular system analgesic, antipyretic, anti-inflammatory bowel diseases (IBD) and anti-tuberculosis drug [11,12].

As a part of our continuous work reporting on the determination of dissociation and stability constants of some organic compounds and their metal complexes by potentiometric techniques [13-16], we report here the proton-ligand dissociation constants of N-Acryloyl-4-aminosalicylic acid (AAS) and its metal stability constants with (Mn²⁺, Co²⁺, Ni²⁺ and Cu²⁺) in monomeric and polymeric forms. Furthermore, the corresponding thermodynamic functions are evaluated and discussed. The geometrical structures of the ligand are carried out by HF method with 3-21G basis set.

Experimental

Materials

All the compounds and solvents used were purchased from Aldrich or Sigma and used as received without further purification. Acryloyl chloride was used without further purification. It was stored below -18°C in a tightly glass-stoppered flask. 2,2'-Azobisisobutyronitrile (AIBN) was used as initiator for all polymerizations. It was purified by

dissolving it in hot ethanol and left to cool. The pure material was being collected by filtration and then dried [17].

Preparation of N-Acryloyl-4-aminosalicylic acid monomer

N-Acryloyl-4-aminosalicylic acid monomer was prepared previously [13] by the reaction of equimolar amounts of acryloyl chloride and 4-aminosalicylic acid in dry benzene until the evolution of hydrogen chloride ceased forming a gray powder of AAS monomer (Figure 1).

Potentiometric studies

N-Acryloyl-4-aminosalicylic acid solution (0.001 M) was prepared by dissolving an accurate weight of the solid in ethanol (AnalaR). Metal ion solutions (0.0001 M) were prepared from AnalaR metal chlorides in bidistilled water and standardized with EDTA [18]. Solutions of 0.001 M (HCl) and 1 M (KCl) were also prepared in bidistilled water. A carbonate-free sodium hydroxide solution in a 20% (by volume) ethanol-water mixture was used as titrant and standardized against oxalic acid (AnalaR).

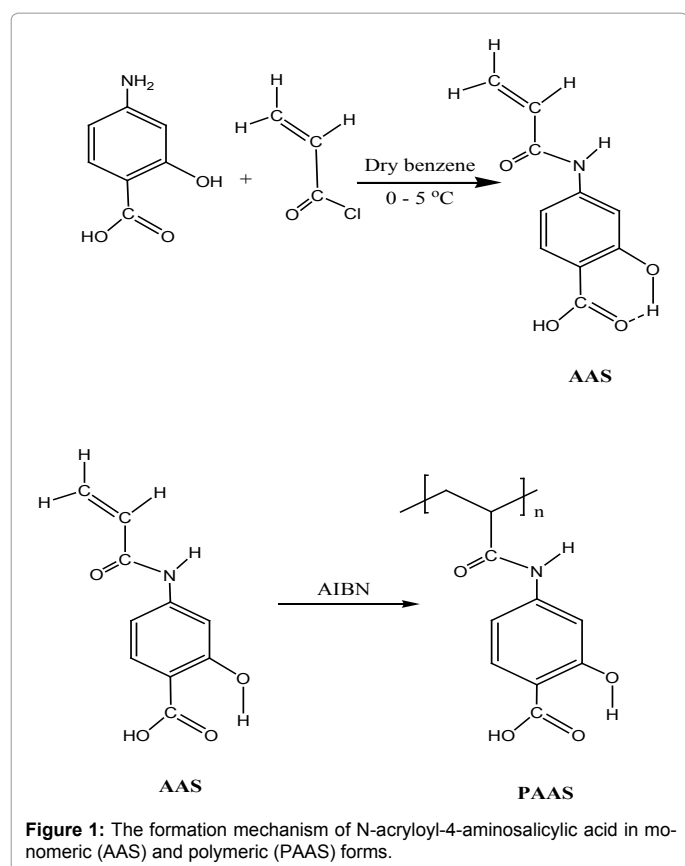
The apparatus, general conditions and methods of calculation were the same as in previous work [13-16]. The following mixtures (i)-(iii) were prepared and titrated potentiometrically at 298 K against standard 0.002 M (NaOH) in a 20% (by volume) ethanol-water mixture:

***Corresponding author:** Chemistry Department, Faculty of Science, Damietta University, Damietta 34517, Egypt Tel: +2 01114266996; E-mail: abinary@yahoo.com

Received August 06, 2014; **Accepted** September 30, 2014; **Published** October 07, 2014

Citation: El-Binary AA, Ghoneim MM, Diab MA, El-Sonbati AZ, Serag LS (2014) Structure, Potentiometric and Thermodynamic Studies of N-Acryloyl-4-amino salicylic acid and Its Metal Complexes in Monomeric and Polymeric Forms. J Thermodyn Catal 5: 135. doi: [10.4172/2157-7544.1000135](https://doi.org/10.4172/2157-7544.1000135)

Copyright: © 2014 El-Binary AA, et al. This is an open-access article distributed under the terms of the Creative Commons Attribution License, which permits unrestricted use, distribution, and reproduction in any medium, provided the original author and source are credited.



- i) 5 cm³ 0.001 M (HCl)+5 cm³ 1 M (KCl)+10 cm³ ethanol.
- ii) 5 cm³ 0.001 M (HCl)+5 cm³ 1 M (KCl)+5 cm³ 0.001 M ligand + 5 cm³ ethanol.
- iii) 5 cm³ 0.001 M (HCl)+5 cm³ 1 M (KCl)+5 cm³ 0.001 M ligand + 10 cm³ 0.0001 M metal chloride + 5 cm³ ethanol.

For each mixture, the volume was made up to 50 cm³ with bidistilled water before the titration. The titrations also were carried out in the presence of 5 ml of AIBN (0.001 M) as initiator for the polymerization step (Figure 1). These titrations were repeated for temperatures of 308 and 318 K. All titrations have been carried out between pH 3.0 and 11.0.

Measurements

Spectroscopic data were obtained using the following instruments: FT-IR spectra (KBr discs, 4000-400 cm⁻¹) by Jasco-4100 spectrophotometer; the ¹H NMR spectrum by Bruker WP 300 MHz using DMSO-d₆ as a solvent containing TMS as the internal standard. The pH measurements were carried out using VWR Scientific Instruments Model 8000 pH-meter accurate to ± 0.01 units. The pH- meter readings in the non-aqueous medium were corrected [19]. The electrode system was calibrated according to the method of Irving et al. [20]. Titrations were performed in a double walled glass cell in an inert atmosphere (nitrogen) at ionic strength of 0.1 M KCl. Potentiometric measurements were carried out at different temperature. The temperature was controlled to within ± 0.05 K by circulating thermostated water (Neslab 2 RTE 220) through the outer jacket of the vessel.

The molecular structures of the investigated compound were optimized by HF method with 3-21G basis set. The molecules were

built with the Perkin Elmer ChemBio Draw and optimized using Perkin Elmer ChemBio 3D software [21,22]. Quantum chemical parameters such as the highest occupied molecular orbital energy (E_{HOMO}), the lowest unoccupied molecular orbital energy (E_{LUMO}) and HOMO-LUMO energy gap (ΔE) for the investigated molecules are calculated.

Results and Discussion

IR spectra of N-Acryloyl-4-aminosalicylic acid

Examination of IR spectrum of the N-Acryloyl-4-aminosalicylic acid (AAS) shows a broad band appears at ~3458 cm⁻¹ corresponding to amide ν_{NH} stretching vibration followed by medium broad band appears at 3006 and 2889 cm⁻¹ which assigned to OH of phenolic, carboxylic OH, respectively [17]. This broadening is an evidence for the presence of weak hydrogen bond between OH and carboxylic groups [23]. IR spectrum of AAS exhibits a bands at 1879 and 1612 cm⁻¹ is assigned to the antisymmetric stretching vibration of carboxylic and amidic carbonyl group, respectively. The bands at 1616, 1569 and 1415 cm⁻¹ are assigned to the (C-H), ν(C=C) and ν(C-C) bands, respectively [24]. The bands in the region 1236-1106 cm⁻¹ are due to the C-H in plane deformation, while the out-of-plane deformation vibration between 727-962 cm⁻¹ and the C-C out-of-plan deformation at 500 cm⁻¹ are assigned.

¹H-NMR spectra

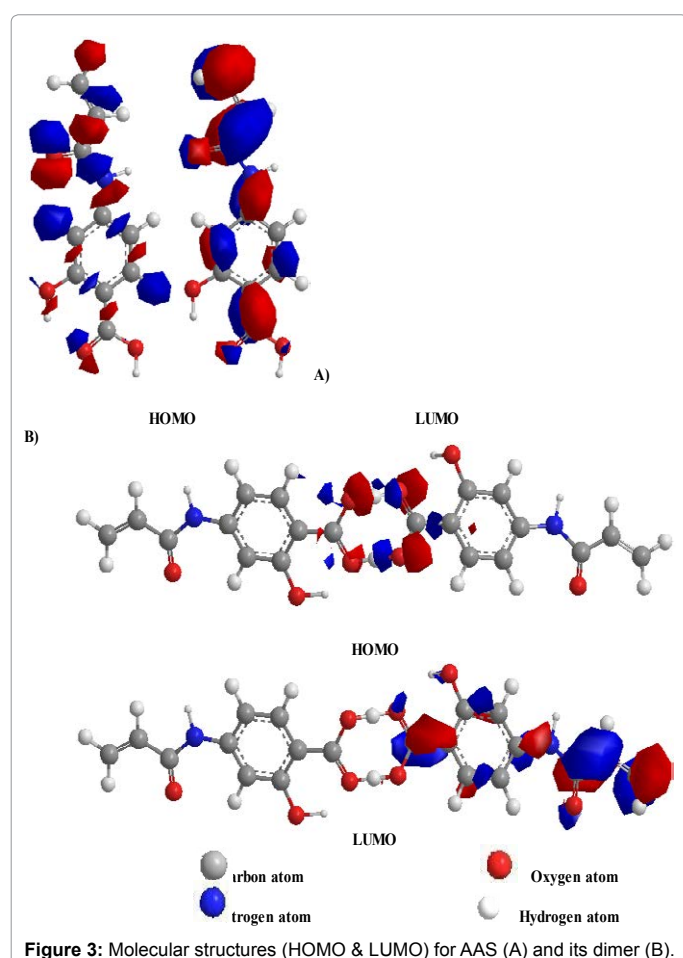
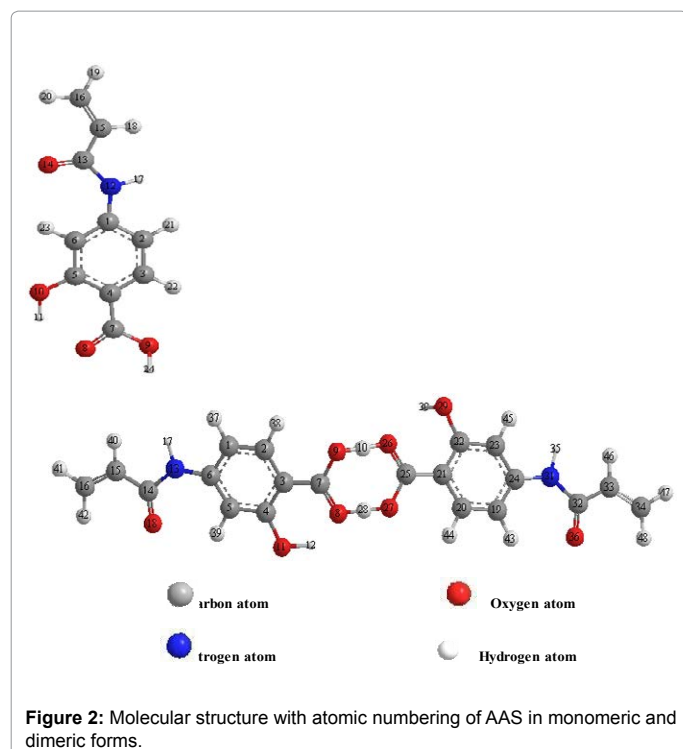
The ¹H NMR spectrum of AAS revealed six resonances at 10.80, 7.57, 7.28, 3.20, 2.53 and 2.10 ppm relative to TMS which may be assigned to an acid group COOH, CONH, aromatic protons, OH phenolic, vinylic -CH- and -CH₂ protons, respectively [25]. The peak at (10.80/3.20/7.57) ppm, which is due to the exchangeable hydrogen-bonded carboxyl/hydroxyl/amine (COOH/OH/NH) proton, respectively which disappears upon exchange with D₂O and can be associated with the COOH/OH/NH protons involved in intramolecular hydrogen bonding. The ¹H NMR spectrum of the ASS monomer showed the expected peaks and pattern of the vinyl group (CH₂=CH) δ 6.82 ppm (dd, J = 17, 11 Hz) for the vinyl CH proton and proton δ 6.32 ppm (AM part of AMX system dd, J = 17, 1 Hz) for the vinyl CH₂ protons, respectively. These peaks disappeared on polymerization while a triplet at δ 2.53 ppm (t, J = 7 Hz) and a doublet at 2.10 ppm (d, J = 7 Hz) appeared, indicating that the polymerization of AAS monomer occurs on the vinyl group [26]. It is worth noting that the rest of the proton spectrum of the monomer and polymer remain almost without change.

Molecular structure

The molecular structures of the N-Acryloyl-4-aminosalicylic acid (AAS) were optimized by HF method with 3-21G basis set. The molecules were built with the Perkin Elmer ChemBioDraw and optimized using Perkin Elmer ChemBio3D software. The calculated molecular structures for AAS are shown in Figure 2. Selected geometric parameters bond lengths and bond angles of AAS are tabulated in Table 1. Molecular structures (HOMO & LUMO) for AAS and its dimeric form are presented in Figure 3.

The HOMO-LUMO energy gap, ΔE, which is an important stability index, is applied to develop theoretical models for explaining the structure and conformation barriers in many molecular systems. The smaller is the value of ΔE, the more is the reactivity of the compound has [21,22,27]. The calculated quantum chemical parameters are given in Table 2.

Additional parameters such as separation energies, ΔE, absolute



electronegativities, χ , chemical potentials, Pi , absolute hardness, η , absolute softness, σ , global electrophilicity, ω , global softness, S , and additional electronic charge, ΔN_{\max} , have been calculated according to the following equations (1-8) [21,22,28]:

$$\Delta E = E_{LUMO} - E_{HOMO} \quad (1)$$

$$\chi = \frac{-(E_{HOMO} + E_{LUMO})}{2} \quad (2)$$

$$\eta = \frac{E_{LUMO} - E_{HOMO}}{2} \quad (3)$$

$$\sigma = \frac{1}{\eta} \quad (4)$$

$$Pi = -\chi \quad (5)$$

$$S = \frac{1}{2\eta} \quad (6)$$

$$\omega = \frac{Pi^2}{2\eta} \quad (7)$$

$$\Delta N_{\max} = \frac{-Pi}{\eta} \quad (8)$$

In the ring part, the CC bond lengths of the benzene rings are observed in the range 1.339 -1.35 Å. The CO bond lengths in the carboxylic acid group conform to the average values are tabulated for an aromatic carboxylic acid in which C=O is 1.229 Å and C-O is 1.349 Å. In AAS, C5-C4-C7 angle is smaller than C3-C4-C7 because of interaction between the carboxyl acid (COOH) and hydroxyl (OH) group (Figure 4A). These results are in agreement with literatures [23,29-31].

The torsional angles C5-C4-C7-O9 and C3-C4-C7-O8 are 178.8° and 179.3°, respectively. The tilt angles are calculated 180°. The dihedral angles are nearly the same among the all conformers. The geometric dimer structure of AAS is also calculated (Figure 2). Stabilization energy lowest value of dimer showed higher stability than AAS. Inter-molecular hydrogen bonds can be responsible for the geometry and the stability of a predominant conformation; the formation of hydrogen bonding between two molecules via a hydroxyl group and -COOH cause the structure of the dimer to be the most stable conformer (Figure 4B). The intermolecular hydrogen bonds are almost linear (the O-H...O angle equals 179.4°) and their length is 2.063 Å. The intramolecular hydrogen bonds between the hydroxyl groups and the oxygen atoms of the carbonyl groups are strongly bent (the O-H...O angle equals 164.7°) and the O...O distance is 2.056 Å [32].

Potentiometric studies

The interaction of a metal with an electron donor atom of a ligand (H_2L) is usually followed by the release of H^+ . Alkaline potentiometric titrations are based on the detection of the protons released upon complexation. The main advantage of this technique, compared to other methods is that from the titration curves it is possible to follow complexation continuously as a function of pH and to detect exactly at which pH complexation takes place. Furthermore, it is possible to calculate the dissociation constants and the stability constants of its

Theoretical			
Bond lengths (Å)			
O(9)-H(24)	0.971	N(12)-C(13)	1.365
C(6)-H(23)	1.098	O(10)-H(11)	1.0
C(3)-H(22)	1.102	C(5)-O(10)	1.379
C(2)-H(21)	1.104	C(7)-O(9)	1.349
O(8)-H(11)	1.007	C(7)-O(8)	1.229
N(12)-C(1)	1.35	C(4)-C(7)	1.366
C(16)-H(20)	1.1	C(6)-C(1)	1.346
C(16)-H(19)	1.102	C(5)-C(6)	1.345
C(15)-H(18)	1.105	C(4)-C(5)	1.35
N(12)-H(17)	1.01	C(3)-C(4)	1.339
C(15)-C(16)	1.342	C(2)-C(3)	1.342
C(13)-C(15)	1.36	C(1)-C(2)	1.348
C(13)-O(14)	1.206		
Bond angles (°)			
H(20)-C(16)-C(15)	122.966	O(9)-C(7)-O(8)	119.333
C(15)-C(13)-O(14)	124.552	O(9)-C(7)-C(4)	125.455
C(15)-C(13)-N(12)	111.542	O(8)-C(7)-C(4)	115.212
O(14)-C(13)-N(12)	123.905	C(7)-C(4)-C(5)	114.09
C(1)-N(12)-H(17)	109.793	C(7)-C(4)-C(3)	124.218
C(1)-N(12)-C(13)	133.388	N(12)-C(1)-C(6)	126.721
H(17)-N(12)-C(13)	116.819	N(12)-C(1)-C(2)	115.026
Torsional angles (°)			
C(5)-C(4)-C(7)-O(9)	178.807		
C(3)-C(4)-C(7)-O(8)	179.382		
Intermolecular H-bond (Dimer)			
Bond lengths(Å)		Bond angles (°)	
O(9)-H(10)	1.010	O(26)-H(10)-O(9)	176.73
H(10)-O(26)	1.075	O(8)-H(28)-O(27)	179.427
O(27)-H(28)	0.991	O(11)-H(12)-O(8)	164.782
H(28)-O(8)	1.072	O(29)-H(39)-O(26)	164.113
O(11)-H(12)	0.995		
H(12)-O(8)	1.061		
O(29)-H(39)	1.003		
O(26)-H(39)	1.073		

Table 1: Selected geometric parameters for N-Acryloyl-4-aminosalicylic acid (AAS) and its dimer form.

complexes from the potentiometric titration

The following equilibria were used for the determination of the pK_a values of H_2L (AAS) (eqs. 9 and 10) and the metal stability constants (eqs. 11 and 12):



Figures 5,6 shows a typical titration curve of the free acid in the absence and presence of compound AAS and its metal ion complexes. It can be seen that for the same volume of NaOH added, the compound titration curves show a lower pH value than the titration curve of free acid. From these titration curves, the average number of protons associated with N-Acryloyl-4-aminosalicylic acid molecule, n_A , in monomeric (AAS) and polymeric (PAAS) forms were determined at

different pH values applying the following Eq. 13:

$$\bar{n}_A = Y \pm \frac{(V_1 - V_2)(N^o + E^o)}{(V^o - V_1)TC_L^o} \quad (13)$$

where Y is the number of available protons in AAS ($Y=2$) and V_1 and V_2 are the volumes of alkali required to reach the same pH on the titration curve of hydrochloric acid and reagent, respectively, V^o is the initial volume (50 cm^3) of the mixture, TC_L^o is the total concentration of the reagent, N^o is the normality of the sodium hydroxide solution and E^o is the initial concentration of the free acid. The titration curves (\bar{n}_A vs pH) for the proton-ligand systems were constructed and found to extend between 0 and 2 on the n_A scale (Figure 7). This means that AAS and PAAS have two dissociable protons (the hydrogen ion of the

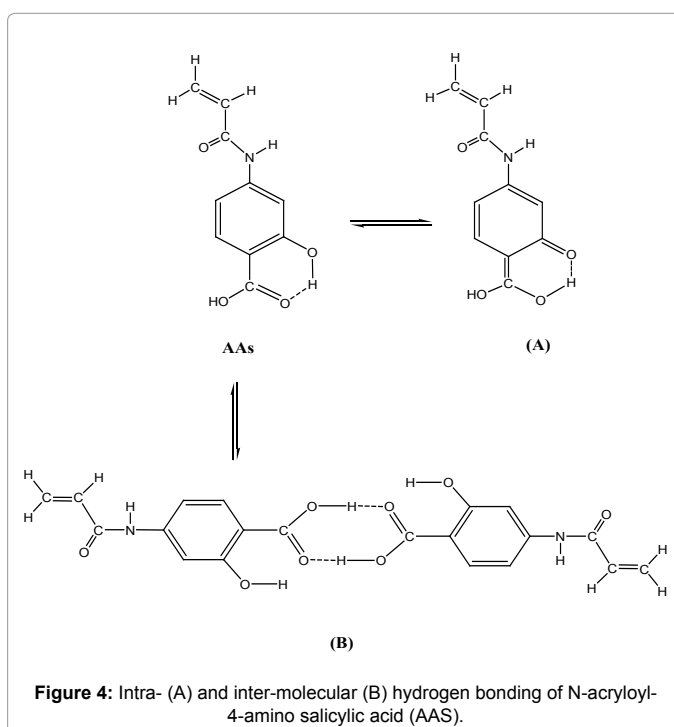


Figure 4: Intra- (A) and inter-molecular (B) hydrogen bonding of N-acryloyl-4-amino salicylic acid (AAS).

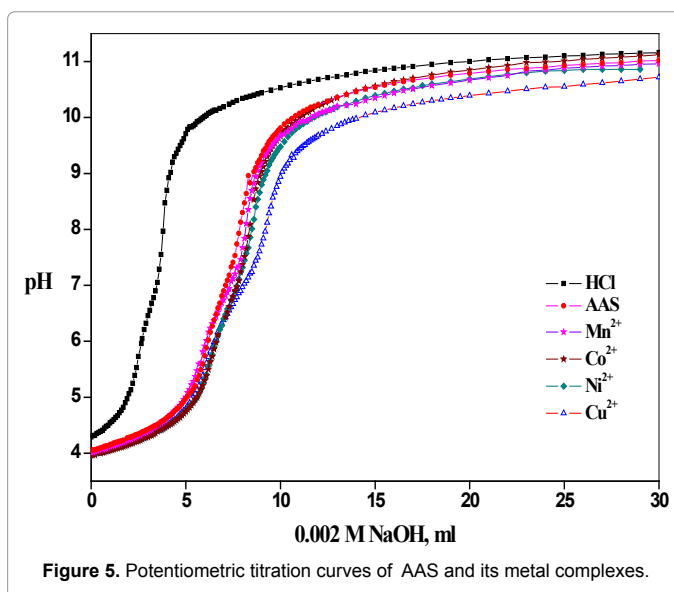


Figure 5: Potentiometric titration curves of AAS and its metal complexes.

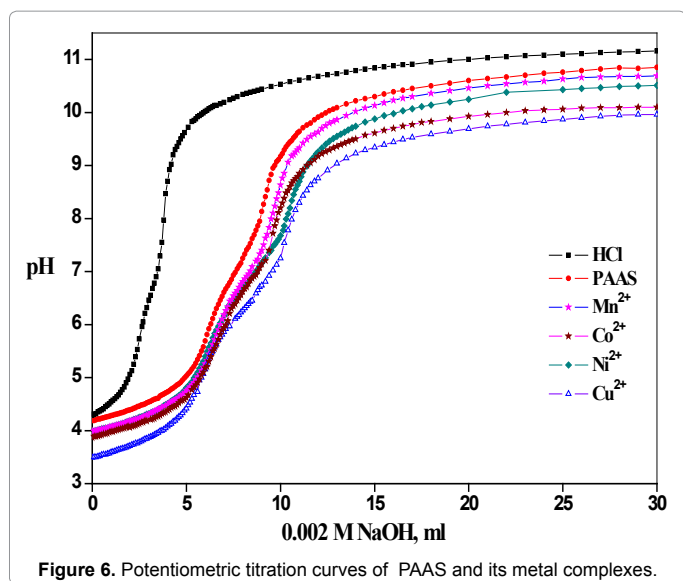


Figure 6. Potentiometric titration curves of PAAS and its metal complexes.

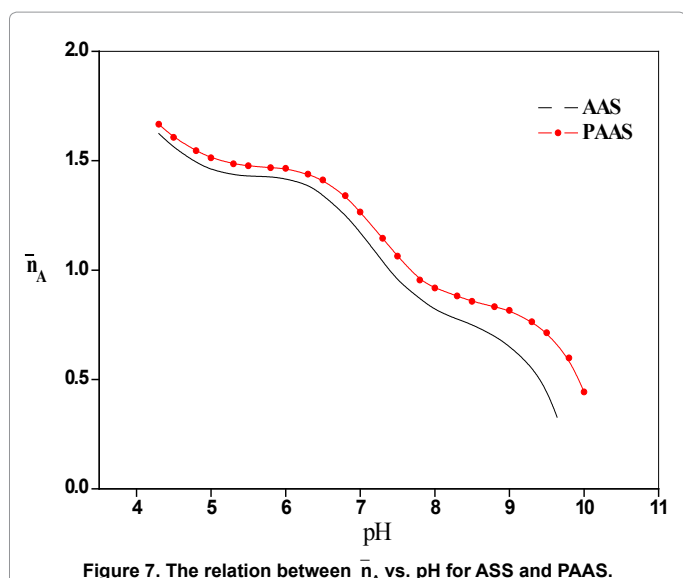


Figure 7. The relation between \bar{n}_A vs. pH for ASS and PAAS.

-OH phenolic moiety, pK_1^H and the COOH group, pK_2^H). Different computational methods [33] were applied to evaluate the dissociation constants. Three replicate titrations were performed; the average values obtained are listed in Table 3. The PAAS has a lower acidic character (higher pK^H values) than AAS. This is quite reasonable because the presence of the vinyl group ($H_2C=CH$) in monomeric form will decrease the electron density, whereby weaker O-H bond is formed. The absence of vinyl group in polymeric form will lead to the opposite effect (i.e., retard the removal of the ligand proton and hence increase the basicity of PAAS).

The formation curves for the metal complexes were obtained by plotting the average number of the ligands AAS and PAAS attached per metal ions (\bar{n}) versus the free ligand exponent (pL), according to Irving and Rossotti [34]. The average number of the reagent molecules attached per metal ion, \bar{n} , and free ligand exponent, pL, can be calculated using the Eqs. 14 and 15:

$$\bar{n} = \frac{(V_3 - V_2)(N^o + E^o)}{(V^o - V_2) \cdot n_A \cdot TC_M^o} \quad (14)$$

and

$$pL = \log_{10} \frac{\sum_{n=0}^{n=J} \beta_n^H \left(\frac{1}{[H^+]} \right)^n}{TC_L^o - n \cdot TC_M^o} \cdot \frac{V^o + V_3}{V^o} \cdot \frac{n!}{r!(n-r)!} \quad (15)$$

where TC_M^o is the total concentration of the metal ion present in the solution, β_n^H is the overall proton-reagent stability constant. V_1 , V_2 and V_3 are the volumes of alkali required to reach the same pH on the titration curves of hydrochloric acid, organic ligand and complex, respectively. These curves were analyzed and the successive stability constants were determined using different computational methods [35,36]. The values of the stability constants ($\log K_1$ and $\log K_2$) are given in Table 4.

The following general remarks can be made:

i) The maximum value of \bar{n} was ~ 2 indicating the formation of 1:1 and 1:2 (metal:ligand) complexes only [37].

ii) The metal ion solution used in the present study was very dilute ($2 \times 10^{-5} M$), hence there was no possibility of formation of metal hydroxide and polynuclear complexes [38,39].

iii) The metal titration curves were displaced to the right-hand side of the ligand titration curves along the volume axis, indicating proton release upon complex formation of the metal ion with the ligand. The large decrease in pH for the metal titration curves relative to ligand titration curves point to the formation of strong metal complexes [40,41].

iv) For all the complexes, the stability constants of PAAS are higher than AAS. This is quite reasonable because the ligand in polymeric forms are better complexing agent [15].

v) For the same ligand (AAS and PAAS) at constant temperature, the stability of the chelates increases in the order Mn^{2+} , Co^{2+} , Ni^{2+} , Cu^{2+} [42 - 44]. This order largely reflects that the stability of Cu^{2+} complexes are considerably larger as compared to other metals of the 3d series. Under the influence of both the polarizing ability of the metal ion [45] and the ligand field [46], Cu^{2+} will receive some extra stabilization due to tetragonal distortion of octahedral symmetry in its complexes. The greater stability of Cu^{2+} complexes is produced by the well known *Jahn-Teller* effect [47].

Effect of temperature

The dissociation constants (pK^H) for ASS and PAAS as well as the stability constants of its complexes with Mn^{2+} , Co^{2+} , Ni^{2+} and Cu^{2+} have been evaluated at (298, 308 and 318) K, and are given in Tables 3, 4. The enthalpy change (ΔH) for the dissociation and complexation process was calculated from the slope of the plot pK^H or $\log K$ vs. $1/T$ using the graphical representation of the van't Hoff Eqs. 16 and 17:

$$\Delta G = -2.303 RT \log K = \Delta H - T \Delta S \quad (16)$$

$$\text{or} \quad \log K = \left(\frac{-\Delta H}{2.303R} \right) \left(\frac{1}{T} \right) + \frac{\Delta S}{2.303R} \quad (17)$$

From the ΔG and ΔH values one can deduce the S using the well known relationships 16 and 18:

$$\Delta S = (\Delta H - \Delta G) / T \quad (18)$$

Comp.	E_{HOMO} (a.u)	E_{LUMO} (a.u)	ΔE (a.u)	χ (a.u)	η (a.u)	σ (a.u) ⁻¹	Pi (a.u)	S (a.u) ⁻¹	ω (a.u)	ΔN_{max}
AAS	-0.348	-0.170	0.178	0.259	0.089	11.223	-0.259	5.6117	0.3755	2.903
Dimer	-0.347	-0.174	0.173	0.260	0.086	11.510	-0.260	5.7554	0.3907	2.999

Table 2 : Stabilization energy of AAS and its dimer, HOMO, LUMO and other additional parameters.

Comp.	Temp. K	Dissociation constant		Free energy change		Enthalpy change		Entropy change	
		pK_1^{H}	pK_2^{H}	ΔG_1	ΔG_2	ΔH_1	ΔH_2	$-\Delta S_1$	$-\Delta S_2$
AAS	298	9.41	4.71	53.69	26.87	32.63	23.58	70.68	9.91
	308	9.24	4.54	54.49	26.77			70.98	9.89
	318	9.05	4.37	55.10	26.60			70.67	9.90
PAAS	298	9.89	5.00	56.43	29.44	29.88	24.50	89.48	13.52
	308	9.72	4.86	57.32	29.36			90.25	13.51
	318	9.64	4.73	58.69	29.28			87.94	13.53

Table 3: Thermodynamic functions for the dissociation of AAS and PAAS in 20% (by volume) ethanol-water mixture in the presence of 0.1 M KCl at different temperatures.

Comp.	M^{n+}	298 K		308 K		318 K	
		log K					
AAS	Mn^{2+}	5.00 ⁻¹	4.20 ⁻²	5.18 ⁻¹	4.37 ⁻²	5.37 ⁻¹	4.56 ⁻²
	Co^{2+}	5.18	4.37	5.35	4.53	5.47	4.71
	Ni^{2+}	5.24	4.43	5.41	4.58	5.52	4.75
	Cu^{2+}	5.44	4.61	5.62	4.79	5.70	4.90
PAAS	Mn^{2+}	7.44	6.41	7.67	6.63	7.89	6.82
	Co^{2+}	7.63	6.59	7.85	6.78	8.06	6.98
	Ni^{2+}	7.72	6.65	7.91	6.86	8.13	7.07
	Cu^{2+}	7.95	6.87	8.14	7.07	8.35	7.26

Table 4: Stepwise stability constants for ML and ML₂ complexes of AAS and PAAS in 20% (by volume) ethanol-water mixture in the presence of 0.1 M KCl at different temperatures.

where $R = 8.314 \text{ J K}^{-1} \text{ mol}^{-1}$ is the gas constant, K is the dissociation constant for the ligand or the stability constant of the complex, and T is absolute temperature.

All thermodynamic parameters of the dissociation process of ASS and PAAS are recorded in Table 3. From these results the following conclusions can be made:

i) The pK^{H} values decrease with increasing temperature, i.e., the acidity of the ligand increase.

ii) A positive value of ΔH indicates that the process is endothermic.

iii) A large positive value of ΔG indicates that the dissociation process is not spontaneous [45].

iv) A negative value of ΔS is obtained due to the increased order as a result of the solvation process.

All the thermodynamic parameters of the stepwise stability constants of AAS and PAAS complexes are recorded in Table 5.

It is known that the divalent metal ions exist in solution as octahedrally hydrated species [36] and the obtained values of ΔH and ΔS can then be considered as the sum of two contributions: (a) release of H_2O molecules, and (b) metal-ligand bond formation. Examination of these values shows that:

i) The stepwise stability constants ($\log K_1$ and $\log K_2$) for AAS and PAAS complexes increases with increasing temperature [48].

ii) The negative value of ΔG for the complexation process of AAS and PAAS suggests the spontaneous nature of such processes [49,50].

iii) The ΔH values of AAS and PAAS are positive, meaning that these processes are endothermic and favourable at higher temperature.

iv) The ΔS values for the complexes of AAS and PAAS are positive, confirming that the complex formation is entropically favourable [14].

Conclusion

N-Acryloyl-4-aminosalicylic acid (AAS) has been synthesized and characterized using spectroscopic techniques (IR and ¹H NMR). The geometrical structures of these ligands are carried out by HF method with 3-21G basis set. The geometric dimer structure more stable than AAS. The protonation constants (pK_1 and pK_2) of the AAS and PAAS were determined by Irving-Rossetti pH titration technique. Also metal-ligand stability constants of their complexes with metal ions (Mn^{2+} , Co^{2+} , Ni^{2+} and Cu^{2+}) have been determined potentiometrically. It appears that PAAS are better complexing agent with metal ions compared to AAS with the order: $\text{Mn(II)} < \text{Co(II)} < \text{Ni(II)} < \text{Cu(II)}$. The corresponding thermodynamic parameters (ΔG , ΔH and ΔS) were derived and discussed. The dissociation process is non-spontaneous,

Comp.	M ⁿ⁺	T/K	free energy change (kJ mol ⁻¹)		Enthalpy change (kJ mol ⁻¹)		Entropy change (J mol ⁻¹ K ⁻¹)	
			- ΔG ₁	- ΔG ₂	ΔH ₁	ΔH ₂	ΔS ₁	ΔS ₂
AAS	Mn ²⁺	298	28.52	23.96	33.55	32.63	208.31	189.91
		308	30.54	25.77			208.11	189.61
		318	32.69	27.76			208.32	189.92
	Co ²⁺	298	29.55	24.93	26.35	30.82	187.60	187.09
		308	31.55	26.71			187.98	186.80
		318	33.30	28.67			187.59	187.10
Ni ²⁺	298	29.89	25.27	25.45	29.00	185.73	182.13	
	308	31.90	27.00			186.21	181.84	
	318	33.61	28.92			185.72	182.14	
Cu ²⁺	298	31.03	26.30	31.63	26.37	210.30	176.75	
	308	33.14	28.24			210.31	177.33	
	318	34.70	29.83			208.60	176.74	
PAAS	Mn ²⁺	298	42.45	36.57	40.82	37.21	279.43	247.59
		308	45.23	39.09			279.39	247.75
		318	48.04	41.52			279.43	247.59
	Co ²⁺	298	43.53	37.60	39.01	35.36	276.99	244.83
		308	46.29	39.98			276.96	244.62
		318	49.07	42.49			276.99	244.84
	Ni ²⁺	298	44.04	37.94	35.36	30.01	266.47	228.03
		308	46.64	40.45			272.07	228.78
		318	49.50	43.04			272.49	229.74
	Cu ²⁺	298	45.36	39.19	36.26	35.38	273.89	250.26
		308	48.00	41.69			273.58	250.24
		318	50.84	44.20			273.90	250.26

Table 5: Thermodynamic functions for ML and ML₂ complexes of AAS and PAAS in 20% (by volume) ethanol-water mixture and 0.1 M KCl.

endothermic and entropically unfavorable. The formation of the metal complexes has been found to be spontaneous, endothermic and entropically favorable.

References

- Nurchi VM, Crespo-Alonso M, Toso L, Lachowicz JI, Crisponi G (2013) Iron^{III} and aluminium^{III} complexes with substituted salicylaldehydes and salicylic acids. *J Inorg Biochem* 128: 174-182.
- Rivas BL, Pereira ED, Moreno-Villoslada I (2003) Water-soluble polymer-metal ion interactions. *Prog Polym Sci* 28: 173-208.
- Ghoneim MM, El-Sonbati AZ, Diab MA, El-Binary AA, Serag LS (2014) Supramolecular Assembly on coordination of azopolymer complexes: A review. *Polym-Plast Technol Eng*
- Elbagerma MA, Azimi G, Edwards HGM, Alattijal AI, Scowen IJ (2010) In situ monitoring of pH titration by raman spectroscopy. *Spectrochim Acta Part A* 75: 1403-1410.
- Lin J, Sahakian DC, Morais SMD, Xu JJ, Polzer RJ et al. (2003) The role of absorption, distribution, metabolism, excretion and toxicity in drug discovery. *Curr Top Med Chem* 3: 1125-1154.
- Acar N, Tulun T (2001) Interaction of polymer-small molecule complex with cupric(II) ions in aqueous ethanol solution. *Europolym J* 37: 1599-1605.
- Rhazia M, Desbrières J, Tolaimatea A, Rinaudob M, Votterod P (2002) Influence of the nature of the metal ions on the complexation with chitosan: Application to the treatment of liquid waste. *Europolym J* 38: 1523-1530.
- Morlay C, Cromer M, Mougnot Y, Vittori O (1998) Potentiometric study of Cu(II) and Ni(II) complexation with two high molecular weight poly(acrylic acids). *Talanta* 45: 1177-1188.
- Morlay C, Cromer M, Mougnot Y, Vittori O (1999) Potentiometric study of Cd(II) and Pb(II) complexation with two high molecular weight poly(acrylic acids); comparison with Cu(II) and Ni(II). *Talanta* 48: 1159-1166.
- Mougnot Y, Morlay C, Cromer M, Vittori O (2003) Potentiometric study of copper(II) and nickel(II) complexation by a cross-linked poly(acrylic acid) gel. *Anal Chim Acta* 407: 337-345.
- Zhao ZB, Zheng HX, Wei YG, Liu J (2007) Synthesis of azo derivatives of 4-aminosalicylic acid. *Chin Chem Lett* 18: 639-642.
- Sheng SF, Zheng HX, Liu J, Zhao ZB (2008) Synthesis of phenol-class azo derivatives of 4-aminosalicylic acid. *Chin Chem Lett* 19: 419-422.
- Ghoneim MM, El-Ghamaz NA, El-Sonbati AZ, Diab MA, El-Binary AA et al. (2015) Optical and thermal properties of azo derivatives of salicylic acid thin films. *Spectrochim Acta A* 137: 1039-1049
- Issa RM, El-Sonbati AZ, El-Binary AA, Kera HM (2002) Polymer complexes XXXIV. Potentiometric and thermodynamic studies of monomeric and polymeric complexes containing 2-acrylamidosulphadiazine. *Europ Polym J* 38: 561-566.
- El-Sonbati AZ, El-Binary AA, El-Deeb NA (2002) Polymer complexes XXXII. Potentiometric and thermodynamic studies of cinnamaldehyde anthranilic acid and its metal complexes in monomeric and polymeric forms. *React Funct Polym* 50: 131-138.
- Issa RM, El-Sonbati AZ, El-Binary AA, Kera HM (2003) Polymer complexes XLIV. Potentiometric and thermodynamic studies of monomeric and polymeric complexes containing 2-acrylamido-2-methylpropanesulfonic acid. *J Inorg Organom Polym* 13: 269-283.
- Khairou KS, Diab MA (1994) Thermal degradation of poly(acryloyl chloride) and copolymers of acryloyl chloride with methyl acrylate. *Polym Deg Stab* 43: 329-333.
- Jeffery GH, Bassett J, Mendham J, Deney RC (1989) Vogel's Textbook of Quantitative Chemical Analysis, 5th Edition. Longman, London.
- Bates RG, Paabo M, Robinson RA (1963) Interpretation of pH measurements in alcohol-water solvents. *J Phys Chem* 67: 1833-1838.
- Irving HM, Miles MG, Pettit LD (1967) A study of some problems in determining the stoichiometric proton dissociation constants of complexes by potentiometric titrations using a glass electrode. *Anal Chim Acta* 38: 475-488.

21. El-Ghamaz NA, Ghoneim MM, El-Sonbati AZ, Diab MA, El-Bindary AA (2014) Synthesis and optical properties studies of antipyrine derivatives thin films. *J Saudi Chem Soc*
22. El-Bindary AA, El-Sonbati AZ, Diab MA, El-Katori EE, Seyam HA (2014) Potentiometric and thermodynamic studies of some Schiff-base derivatives of 4-aminoantipyrine and their metal complexes. *Int J Adv Res* 2: 493-502.
23. Takahashi M, Ishikawa Y, Ito H (2012) The dispersion correction and weak-hydrogen-bond network in low-frequency vibration of solid-state salicylic acid. *Chem Phys Lett* 531: 98-104.
24. Diab MA (1994) Thermal stability of poly homopolymer and copolymers of acryloyl chloride with methyl acrylate. *Acta Polym* 41: 731-738.
25. El-Sonbati AZ, Belal AAM, El-Wakeel SI, Hussien MA (2004) Stereochemistry of new nitrogen containing heterocyclic compounds X. Supramolecular structures and stereochemical versatility of polymeric complexes. *Spectrochim Acta A* 60: 965-972.
26. El-Sonbati AZ, El-Bindary AA, Diab MA (2003) Polymer complexes XXXX. Supramolecular assembly on coordination models of mixed-valence-ligand poly [1-acrylamido-2-(2-pyridyl)ethane] complexes. *Spectrochim Acta A* 59: 443-454.
27. El-Ghamaz NA, El-Sonbati AZ, Diab MA, El-Bindary AA, Awad MK (2014) Dielectrical, conduction mechanism and thermal properties of rhodanine azodyes. *Mater Sci Semicond Process* 19: 150-162.
28. El-Sonbati AZ, Diab MA, El-Bindary AA, Morgan SM (2014) Supramolecular spectroscopic and thermal studies of azodye complexes. *Spectrochim Acta A* 127: 310-328.
29. Kivelson D, Niemen R (1961) ESR studies on the bonding in copper complexes. *J Chem Phys* 35: 149-155.
30. Karabacak M, Kurt M (2009) The spectroscopic (FT-IR and FT-Raman) and theoretical studies of 5-bromo-salicylic acid. *J Mol Struct* 919: 215-222.
31. Karabacak M, Kose E, Kurt M (2010) FT-Raman, FT-IR spectra and DFT calculations on monomeric and dimeric structures of 5-fluoro- and 5-chloro-salicylic acid. *J Raman Spectroscopy* 41: 1085-1097.
32. Boczar M, Boda L, Wójcik MJ (2006) Theoretical modeling of infrared spectra of hydrogen bonded crystals of salicylic acid. *Spectrochim Acta A* 64: 757-760.
33. Irving H, Rossotti HS (1954) The calculation of formation curves of metal complexes from pH titration curves in mixed solvents. *J Chem Soc* 2904-2910.
34. Irving H, Rossotti HS (1953) Methods for computing successive stability constants from experimental formation curves. *J Chem Soc* 3397-3405.
35. Rossotti FJC, Rossotti HS (1955) Graphical methods for determining equilibrium constants. I. Systems of mononuclear complexes. *Acta Chem Scand* 9: 1166-1176.
36. Beck MT, Nagybal I (1990) *Chemistry of Complex Equilibrium*, Wiley, New York.
37. Boraei AAA, Mohamed NFA (2002) Equilibrium studies of ternary systems involving divalent transition metal ions, aliphatic acids and triazoles. *J Chem Eng Data* 47: 987-991.
38. Sanyal P, Sengupta GP (1990) Potentiometric studies of complex-formation of some trivalent rare-earths with p,p'-bromosulphonosalicylidene. *Anil J Ind Chem Soc* 67: 342-346.
39. Sridhar S, Kulanthipandi P, Thillaiarasu P, Thanikachalam V, Manikandan G (2009) Protonating and chelating efficiencies of some biologically important thiocarbonohydrazides in 60 % (v/v) ethanol-water systems by potentiometric and spectrophotometric methods. *J Chem* 4: 133-140.
40. Athawale VD, Lele V (1996) Stability constants and thermodynamic parameters of complexes of lanthanide ions and (\pm)-norvaline. *J Chem Eng Data* 41: 1015-1019.
41. Athawale VD, Nerkar SS (2000) Stability constants of complexes of divalent and rare earth metals with substituted salicylnals. *Monatsh Chem* 131: 267-276.
42. Tirkistani FAA, El-Bindary AA (2005) Potentiometric and thermodynamic studies of rhodanineazosulfonylazide and its metal complexes. *Bull Electrochem* 21: 265-269.
43. Ibañez GA, Escandar GM (1998) Complexation of cobalt(II), nickel(II) and zinc(II) ions with mono and binucleating azo compounds: A potentiometric and spectroscopic study in aqueous solution. *Polyhedron* 17: 4433-4441.
44. Malik WU, Tuli GD, Madan RD (1984) *Selected Topics in Inorganic Chemistry*, 3rd Edition, Chand S. & Company LTD, New Delhi.
45. Harly FR, Burgess RM, Alcock RM (1980) *Solution Equilibria*, p. 257. Ellis Harwood, Chichester.
46. Orgel LE (1966) *An introduction to transition metal chemistry ligand field theory*, p. 55. Methuen, London.
47. Bebot-Bringaud A, Dange C, Fauconnier N, Gerard C (1999) NMR, potentiometric and spectrophotometric studies of phytic acid ionization and complexation properties toward Co²⁺, Ni²⁺, Cu²⁺, Zn²⁺ and Cd²⁺. *J Inorg Biochem* 75: 71-78.
48. Al-Sarawy AA, El-Bindary AA, El-Sonbati AZ, Omar TY (2005) Potentiometric and thermodynamic studies of 3-(4-methoxyphenyl)-5-azorhodanine derivatives and their metal complexes with some transition metals XIV. *Chem Pap* 59: 261-266.
49. Mubarak AT, El-Sonbati AZ, El-Bindary AA (2004) Potentiometric and conductometric studies on the complexes of some transition metals with rhodanine azosulfonamide derivatives XI. *Chem Pap* 58: 320-323.
50. Bhesaniya KD, Baluja S (2014) potentiometric determination of dissociation constant and thermodynamic parameters of dissociation process of some newly synthesized pyrimidine derivatives in MeOH/DMF-water medium at different temperatures. *J Mol Liq* 190: 190-195.